The hemoglobins of the trematodes *Fasciola hepatica* and *Paramphistomum epiclitum*: A molecular biological, physico-chemical, kinetic, and vaccination study

SYLVIA DEWILDE,[1] A. IULIA IOANITESCU,[2] LAURENT KIGER,[3] KAMBIZ GILANY,[1] MICHAEL C. MARDEN,[3] SABINE VAN DOORSLAER,[2] JOZEF VERCRUYSSE,[4] ALESSANDRA PESCE,[5] MARCO NARDINI,[6] MARTINO BOLOGNESI,[6] AND LUC MOENS[1]

[1]Department of Biomedical Science, University of Antwerp, Universiteitsplein 1, B-2610 Antwerp, Belgium
[2]Department of Physics, University of Antwerp, Universiteitsplein 1, B-2610 Antwerp, Belgium
[3]Institut National de la Santé et de la Recherché Médicale (INSERM), Unité U779, 94276 Le Krêmlin-Bicêtre, France
[4]Department of Virology, Parasitology, and Immunology, Faculty of Veterinary Medicine, Ghent University, 9820 Merelbeke, Belgium
[5]Department of Physics, CNISM and Centre of Excellence for Biomedical Research, University of Genova, 16136 Genova, Italy
[6]Department of Biomolecular Sciences and Biotechnology, CIMAINA and CNR-INFM, University of Milano, 20133 Milano, Italy

(RECEIVED May 20, 2008; FINAL REVISION June 19, 2008; ACCEPTED June 20, 2008)

Abstract

The trematode *Fasciola hepatica (Fa.he.)* is a common parasite of human and livestock. The hemoglobin (Hb) of *Fa.he*., a potential immunogen, was chosen for characterization in the search for an effective vaccine. Characterization of trematode Hbs show that they are intracellular single-domain globins with the following remarkable features: (1) *Fa.he*. expresses two Hb isoforms that differ at two amino acid sites (F1: 119Y/123Q; F2: 119F/123L). Both isoforms are monoacetylated at their N-termini; (2) the genes coding for *Fa.he*. and *Paramphistomum epiclitum* (*Pa.ep*.) Hbs are interrupted by two introns at the conserved positions B12.2 and G7.0.; (3) UV/VIS and resonance Raman spectroscopy identify the recombinant *Fa.he*. HbF2 as a pentacoordinated high-spin ferrous Hb; (4) electron paramagnetic resonance spectroscopy of cyano-met *Fa.he*. HbF2 proves that the endogenously bound imidazole has no imidazolate character; (5) the major structural determinants of the globin fold are present, they contain a TyrB10/TyrE7 residue pair on the distal side. Although such distal-site pair is a signature for high oxygen affinity, as shown for *Pa.ep*. Hb, the oxygen-binding rate parameters for *Fa.he*. Hb are intermediate between those of myoglobin and those of other trematode Hbs; (6) the three-dimensional structure of recombinant *Fa.he*. HbF2 from this study closely resembles the three-dimensional structure of *Pa.ep*. determined earlier. The set of distal-site polar interactions observed in *Pa.ep*. Hb is matched with small but significant structural adjustments; (7) despite the potential immunogenic character of the fluke Hb, vaccination of calves with recombinant *Fa.he*. HbF2 failed to promote protection against parasitic infection.

Keywords: hemoglobins; fluke; ligand binding; 3D structure; spectroscopy; vaccination

Supplemental material: see www.proteinscience.org

Reprint requests to: Sylvia Dewilde, Department of Biomedical Sciences, University of Antwerp, Universiteitsplein 1, B-2610 Antwerp, Belgium; e-mail: sylvia.dewilde@ua.ac.be; fax: 32-3820-2339.

Abbreviations: Hb, hemoglobin; Mb, myoglobin; *Pa.ep*., *Paramphistomum epiclitum*; *Fa.he*., *Fasciola hepatica*; RMSD, root mean square deviation; RR, resonance Raman; CW-EPR, continuous-wave electron paramagnetic resonance; ESI-MS, electron spray ionization mass spectrometry; HS, high spin; LS, low spin; HALS, highly anisotropic low spin.

Article and publication are at http://www.proteinscience.org/cgi/doi/10.1110/ps.036558.108.

Trematodes are parasites inhabiting various vertebrate body organs such as the bile duct or the stomach of ruminants, where oxygen supply is scarce and intermittent. Liver fluke disease hits agricultural animals such as cattle and sheep, and has a worldwide distribution often resulting in large economic losses. *Fasciola hepatica* (Platyhelminthes, Trematoda; *Fa.he*.) besides being an animal pathogen, is also a major human pathogen (Spithill et al. 2002).

Most trematodes host cytoplasmic hemoglobins (Hb) with a length of ~150 amino acids (~17 KDa). The Hb of *Paramphistomum epiclitum* (*Pa.ep*.), so far the best characterized of trematode Hbs, is monomeric and displays the major determinants of the typical globin fold (Rashid et al. 1997; Kiger et al. 1998; Pesce et al. 2001; Das et al. 2006). The heme-ligand binding site displays a TyrB10/TyrE7 distal residue pair, and a high oxygen affinity (P_{50} < 0.001 mm Hg). Such functional property relies primarily on a very slow O_2-dissociation process linked to a hydrogen-bonding network stabilizing the heme-bound ligand. The network involves TyrB10, a distal-site-trapped water molecule, ThrE10, and the carbonyl group of TyrE7. The TyrE7 side chain, however, is locked next to the CD globin region in a conformation unsuitable for stabilization of the heme-bound ligand (Zhang et al. 1997; Kiger et al. 1998; Pesce et al. 2001; Das et al. 2006).

The physiological roles of trematode Hbs are a matter of debate. Indeed, adult parasitic trematodes and nematodes, e.g., *Ascaris suum*, live mainly in a semi-anaerobic environment; their Hbs display such high oxygen affinities that they cannot simply serve in O_2 transport to the tissues. Therefore, other functions for these Hbs, such as oxygen scavenging, heme reserve for egg production, and NO dioxygenase have been proposed (Goldberg 1995; Rashid et al. 1997; Minning et al. 1999; Rashid and Weber 1999; de Guzman et al. 2007). In addition, they may be involved in host–parasite interactions. Indeed, parasitic trematodes and nematodes are known to secrete/excrete a set of proteins (ES proteins) into the host (Cervi et al. 1996; Berasain et al. 2000). Among these, hemoglobin-like proteins have been identified (McGonigle and Dalton 1995; Dalton et al. 1996). The ES proteins, including Hbs, are potent antigens potentially useful in eliciting host immunological resistance against the parasitic infection through vaccination (Lightowlers and Rickard 1988; Jefferies et al. 1997). McGonigle and Dalton (1995) described the isolation of a hemoprotein with the spectral characteristics of Hb (Mr > 200 kDa) from the ES products of *Fa.he*. A vaccine trial in cattle with this Hb fraction resulted in a 43.8% protection level against fluke infection (Dalton et al. 1996). Therefore, trematode Hbs appear as important, so far scarcely characterized targets for new vaccination strategies. However, it must be noted that vaccination with a given antigen will not necessarily result in protection against the parasitic infection. Indeed, antibodies may not play a key role in the protective effect elicited, because protection may be due to a combination of humoral and cell-mediated responses (Verity et al. 2001).

We present here a molecular, physicochemical, structural, and ligand-binding kinetic characterization of the recombinant Hbs of the trematodes *Fa.he*. and *Pa.ep*. together with their application to a vaccination trial exploring the protective efficacy against a challenge parasite infection.

Results

Structure of trematode globin coding genes

The cDNA and gDNA sequences coding for the *Fa.he*. HbF2 and *Pa.ep*. Hb were determined (accession nos. EU124670, AF113510). The coding sequences of both globin genes are interrupted by two small introns (*Fa.he*. HbF2 gene: 109 base and 249 base; *Pa.ep*. globin gene: 155 base and 424 base). The standard donor and acceptor sequences are present. Using Southern hybridization, at least two globin genes were identified in the genome of *Pa.ep*. (data not shown). This is in keeping with the report by Rashid et al. (1997), that several globin isoforms could be distinguished by isoelectrofocusing in extracts of this species. Based on the alignment of the trematode globin sequences in Figure 1, it can be concluded that the genes are interrupted by introns at the positions B12.2 and G7.0. Such conserved intron location in the globin genes of the evolutionary, very primitive, trematodes is in strong contrast to the intron location observed in nematode globin genes. Indeed, in *Caenorhabditis elegans*, introns are inserted both in conserved positions and in totally new positions (Hoogewijs et al. 2004). The trematode intron pattern is in accordance with the hypothesis that the B12.2 and G7.0 introns in globin genes are ancestral, being the result of the formation of the globin gene from smaller identities itself (intron early hypothesis) (Gilbert 1987), whereas the introns at other positions in the globin genes are most likely the results of later genetic events (intron late hypothesis) (Cavalier-Smith 1985; for review, see Roy and Gilbert 2006).

Primary structure of Fasciola hepatica *hemoglobins and expression cloning*

ESI-MS of the native *Fa.he*. Hb ($n = 4$) revealed the presence of two major components, F1 (16,633.0 ± 0.3 Da; 68%) and F2 (16,602.0 ± 0.3 Da; 32%) (Supplemental Figs. S1, S2). Two peptides in the tryptic digest were found whose mass difference (31 Da) corresponds with the mass difference between the intact chains, F1

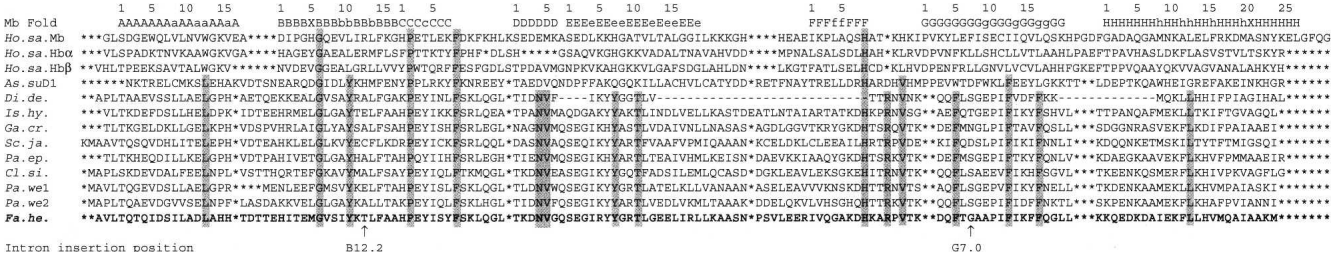

Figure 1. Alignment of trematode globin sequences with sequences of known tertiary structure. *Ho.sa*.Mb, *Homo sapiens* Mb (NP005359); *Ho.sa*.Hbα, *Homo sapiens* Hbα (P69905); *Ho.sa*.Hbβ, *Homo sapiens* Hbβ (P68871); *As.suD1*, *Ascaris suum* Hb domain 1 (1ASH); *Pa.ep*., *Paramphistomum epiclitum* Hb (1H97B); *Di.de*, *Dicreocoelum dendriticum* Hb (P56532); *Ga.cr*., *Gastrothylax cruminifer* Hb; *Is.hy*., *Isoparorchis hypselobagri* Hb (P80722); *Sc.ja*., *Schistosoma japanicum* Hb (AAP06216); *Pa.we.1*, *Paragonimus westermani* Hb1 (AAX11352); *Pa.we.2*, *Paragonimus westermani* Hb1 (AAX11353); *Cl.si*., *Clonorchis sinensis* Hb (AAM18464); *Fa.he*., *Fasciola hepatica* Hb (EU124670). The accession numbers given are from NCBI. (*) Alignment purpose; (−) missing residues; (→) intron insertion position. Positions identical in all trematode globin sequences are highlighted.

and F2. The masses and tandem mass spectra of these peptides are consistent with the sequences YFQGQLK (HbF1) and FFQGLLK (HbF2) (Supplemental Fig. S2). The N termini of both Hbs F1 and F2 are monoacetylated (42.1 Da difference in mass of the N-terminal peptide of *Fa.he*. globins obtained experimentally and calculated from their sequences; Supplemental Fig. S1). The complete primary structures of *Fa.he*. HbF1 and HbF2, determined at the protein level, were reconstructed from relevant peptides (Supplemental Fig. S3). The presented primary structure of *Fa.he*. HbF2 is confirmed by sequencing the corresponding cDNA (accession no. EU124670).

Fa.he. HbF2 was expressed in *Escherichia coli* as described in the Materials and Methods section. In contrast to *Pa.ep*. Hb, which is readily expressed as Hb in the cytosol (Pesce et al. 2001), the *Fa.he*. HbF2 is not folded properly in the *E. coli* system. Heme-lacking globin chains are released in the cytosolic fraction, most likely due to the overexpression. However, in vitro addition of hemin to the isolated extract refolds the recombinant Hb molecule, which can be purified further by standard methods (Dewilde et al. 2001; Pesce et al. 2001).

Kinetics of Fasciola hepatica *hemoglobin*

The O_2- and CO-binding kinetics of *Fa.he*. Hbs were determined by flash photolysis and compared with those of other trematode and standard Hbs (see Fig. 5; Table 1). The O_2 affinity (P_{50} = 0.03 torr) is intermediate between those of sperm whale Mb and of other trematodes.

Spectroscopic characterization of Fasciola hepatica *hemoglobin F2*

Figures 2–4 and Supplemental Figures S4–S6 give the UV/VIS, RR, and CW-EPR spectra for *Fa.he*. HbF2 compared with those of *Pa.ep*. Hb. The spectra are further analyzed in the Discussion section.

Table 1. *Kinetic constants of O_2 and CO reactions with some selected hemoglobins/myoglobins*

Species	Residue B10	Residue E7	k_{on} ($M^{-1}s^{-1}$) $\times 10^{-6}$	k_{off} (s^{-1})	KO_2 (M) $\times 10^8$	l_{on} ($M^{-1}s^{-1}$) $\times 10^{-6}$	l_{off} (s^{-1})	KCO (M) $\times 10^8$	KO_2/KCO	References
Physeter (SW) Mb	Leu	His	15	14	93	0.55	0.019	3.4	27	(Carver et al. 1992)
Mutant SW Mb	Phe	His	21	1.4	6.7	0.22	0.006	2.7	2.4	(Carver et al. 1992)
Ascaris Hb	Tyr	Gln	2.8	0.013	0.36	0.3	-	-	-	(De Baere et al. 1994)
Mutant *Ascaris* Hb	Leu	Gln	9	5	45	0.75	-	-		(De Baere et al. 1994)
Mutant *Ascaris* Hb	Phe	Gln	40	2	5	2.7	-	-	0.090	(De Baere et al. 1994)
Paramphistomum epi.	**Tyr**	**Tyr**	**108**	**0.033**	**0.03**	**28**	-	-	-	(Rashid et al. 1997)
Gastrothylax crum.	**Tyr**	**Tyr**	**205**	**0.4**	**0.19**	**73**	**1.2**	**1.6**	**0.119**	(Kiger et al. 1998)
Explanatum exp.	**?**	**?**	**120**	**0.4**	**0.33**	**33**	**1.2**	**3.6**	**0.092**	(Kiger et al. 1998)
***Dicrocoelium* Hb**	**Tyr**	**Tyr**	**300**	**30**	**10**	**110**	**0.65**	**0.059**	**17**	(Di Iorio et al. 1985)
Fasciola	**Tyr**	**Tyr**	**45**	**2.1**	**4.7**	**15**	-	-	-	This study
LegHb	Tyr	His	116	5.5	4.8	13	0.01	0.0078	61	(Appleby 1962)
Chironomus Hb	Leu	His	300	218	73	0.27	0.095	35	2	(Amiconi et al. 1972)

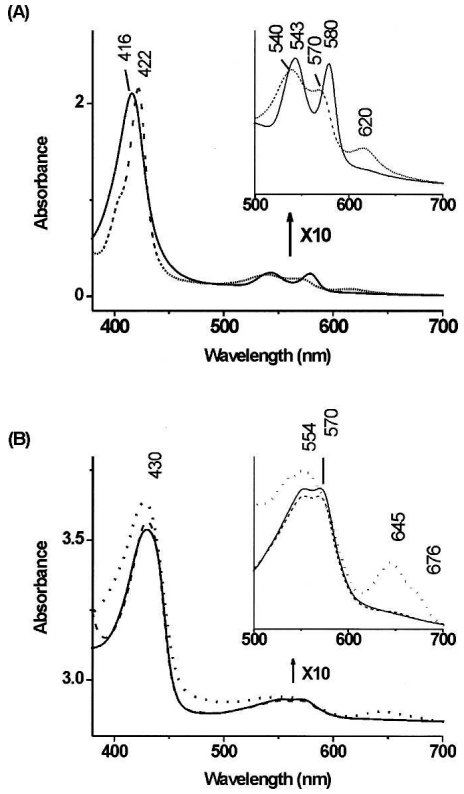

Figure 2. Absorption spectra of *Fasciola hepatica* hemoglobin. (*A*) The oxy form (solid line) and the CO-ligated ferrous form (dashed line) of *Fa.he*. HbF2.; (*B*) the ferrous *Fa.he*. HbF2 at pH 5.5 (solid line), pH 6.8 (dashed line), and pH 10 (dotted line).

Crystal structure analysis

The X-ray crystal structure of *Fa.he*. HbF2 was solved by molecular replacement and refined at 1.8 Å resolution ($R_{factor} = 18.2\%$, $R_{free} = 22.5\%$), with ideal stereochemical parameters (Supplemental Table S1). The typical 8-helix globin fold can be immediately recognized in *Fa.he*. HbF2; the RMSD between the protein backbones of *Fa.he*. HbF2 and of *Pa.ep*. Hb (the molecular replacement model) (Pesce et al. 2001) is 1.04 Å, calculated over 142 C_α pairs.

Vaccination with Fasciola hepatica *hemoglobin*

An experiment was set up in order to test whether a protection against the parasitic infection could be obtained by vaccination with recombinant *Fa.he*. Hb as described in Materials and Methods. Table 2 clearly shows that no protection against *Fa.he.* infection was obtained.

Discussion

The occurrence of two Hb isoforms, F1 and F2, in *Fa.he*. is in accordance with observations in other trematode species, all showing different Hb isoforms (Rashid et al. 1997; Rashid and Weber 1999; de Guzman et al. 2007). Beside *Fa.he*. Hbs, an acetylated N terminus has also been reported for the trematode *Gastrotylax cruminifer* Hb (Das et al. 2006). Acetylated N termini are, in general, scarce in nonvertebrate Hbs, and it is currently not known whether the functional significance of such modification is simply that of protecting the protein in the cytosolic compartment against proteolytic degradation. Our data, however, differ completely from those reported by McGonigle and Dalton (1995) describing *Fa.he*. Hb as a molecule of >200 kDa, with an N-terminal sequence: SEESREKIREGGKMVKAIRD.

The primary structures of *Fa.he*. HbF2 and other trematode globins are aligned with globin sequences of known tertiary structure in Figure 1. Inspection of the aligned sequences immediately shows that the major determinants of the globin fold are conserved (Bashford et al. 1987) and that characteristic sequence signatures of trematode globins can be recognized: (1) a TyrB10/TyrE7 distal residue pair; (2) a high sequence identity in the CD/D region, as well as in the middle of the G-helix (Rashid et al. 1997; Das et al. 2006). Hbs with a TyrB10/TyrE7 pair are known in man as nonfunctional mutants. In trematodes, however, they are linked to (extremely) high oxygen affinity, characterized by very high oxygen association rates (k_{on}) and low dissociation rates (k_{off}), due to stabilization of the heme ligand by a distal-site hydrogen-bonded network (Kiger et al. 1998; Pesce et al. 2001). While the residues building such distal-site network are essentially conserved in *Fa.he*. HbF2, compared with other trematode Hbs the observed oxygen-association rate is lower and the dissociation rate much higher, leading to an oxygen affinity ($P_{50} = 0.03$ torr) nearly an order of magnitude lower. Note that this affinity is still

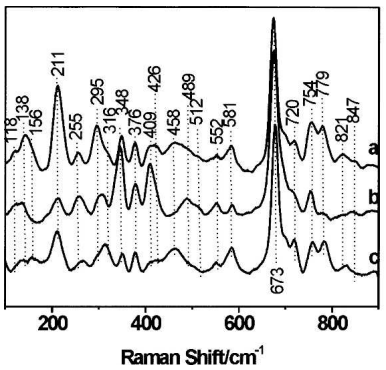

Figure 3. Low-frequency part of the resonance Raman spectra of ferrous deoxy form of *F. hepatica* hemoglobin F2 at pH 5.5 (a) and 6.8 (b), compared with the ferrous deoxy form of wild-type *P. epiclitum* hemoglobin (pH 6.2) (c) (100–900 cm^{-1} region). The laser-excitation wavelength was 413.1 nm at 17 mW power.

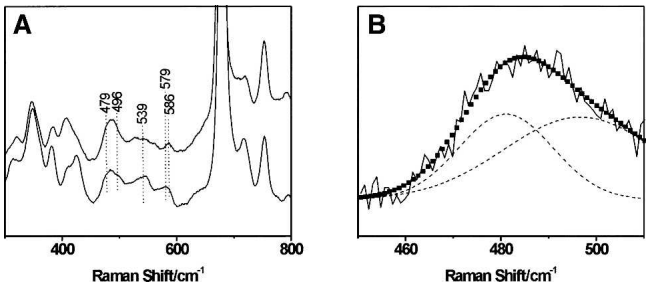

Figure 4. Comparitive resonance Raman spectra of the CO complexes of ferrous *F. hepatica* and *P. epiclitum* hemoglobin. The laser-excitation wavelength was 413.1 nm at 1 mW power. (*A*) Low-frequency spectrum (300–800 cm^{-1}) of *Fa. he*. HbF2CO (*top*) and *Pa.ep*. HbF2CO (*bottom*). (*B*) Detail of the determined RR spectrum of *Fa.he*. HbF2CO (solid black line), the deconvolution into two separate Fe-CO stretching contributions (dashed black line), and the fitted peak (■).

10 times higher than that of sperm whale Mb, taken as a reference globin. *Fa.he*. HbF2 affinity for oxygen is thus nearly halfway (logarithmically) between those of classical vertebrate globins and those of high-affinity trematode Hbs.

Spectroscopic characterization of Fasciola hepatica *hemoglobin F2*

The optical spectrum of *Fa.he* HbF2 in its as-purified form exhibits absorbance maxima at 416, 543, and 580 nm, typical for a ferrous-oxy form of the protein (Fig. 2A; Dewilde et al. 1998; Das et al. 2000). The peak observed around 620 nm suggests the presence of ferryl and/or denatured forms of the protein. The tail around 630 nm indicates that a small fraction of the protein is also in a high-spin (HS) ferric form. This was confirmed by the CW-EPR spectrum of the as-purified sample, which is dominated by contributions of two HS ferric complexes (Supplemental Fig. S4). Given the small fraction of ferric *Fa.he*. HbF2 in the as-purified sample, it is unclear whether the two HS forms are related to the native ferric form(s). The EPR spectrum of ferric cyanide-ligated *Fa.he*. HbF2 revealed a single feature at $g_{max} = 3.445$ (Supplemental Fig. S5). This value is similar to the one found for cyano-met Mb ($g_{max} = 3.45$) (Peisach et al. 1971), but is larger than that of cyanide-ligated ferric horseradish peroxidase ($g_{max} = 3.05$) (Blumberg et al. 1968), indicating that the endogenously bound imidazole has a neutral and not an imidazolate character.

Figure 2B shows the pH dependence of the optical spectra of the ferrous deoxy form of *Fa.he*. HbF2 obtained after addition of dithionite to the sample. The bands at 430 and around 554 nm are typical of a pentacoordinated ferrous heme complex. This was confirmed in the RR spectra by the observation of the ν_4 and ν_3 bands at 1353 cm^{-1} and 1469 cm^{-1}, respectively (Supplemental Fig. S6). The broad band exhibited by deoxy Hb's in the visible region may shelter two or more transitions, as was also previously observed for other trematode globins (Rashid et al. 1997). The presence of a peak at ~645 nm at alkaline pH 10, characteristic of heme degradation, proves large protein instability at this pH. The low-frequency region of the RR spectra of the ferrous deoxy form of *Fa.he*. HbF2 at pH 5.5 and 6.8 are depicted in Figure 3 (lines a and b). As a comparison, the RR spectrum of the ferrous deoxy form of *Pa.ep*. Hb at pH 6.2 is shown in Figure 3 (line c). The corresponding spectrum of *Pa.ep*. Hb at pH 7.4 was shown earlier (Das et al. 2006). The Fe-His stretching vibration ($\nu_{Fe\text{-}His}$) of hemoproteins is a sensitive probe of the heme vicinity and can be influenced by both hydrogen bonding to the proximal histidine and out-of-plane characteristics of the heme iron. The $\nu_{Fe\text{-}His}$ mode of deoxy *Fa.he*. HbF2 is found at 211 cm^{-1}. This compares with the $\nu_{Fe\text{-}His}$ mode of *Pa.ep*. Hb (210 cm^{-1}) (Fig. 3, line c). Earlier, Das et al. (2006) reported values in the same range for *Gastrothylax crumenifer* Hb and *Pa.ep*. Hb, suggesting similar conformation of the heme pocket, as it would be expected from the amino acid sequence comparison (Fig. 1). Still, this value is smaller than the one found in mammalian Hbs and Mbs (~220 cm^{-1}) (Hu et al. 1996). This difference indicates an altered orientation of the proximal histidine imidazole, which is confirmed by the crystal structure analysis. Indeed, it was shown that as the value of the Fe-His stretching vibration decreases, the proximal histidine adopts a more tilted conformation (Das et al. 2004) and a larger out-of-plane distortion is observed (Stavrov 1993).

There is a marked difference between the in-plane and out-of-plane modes in the low-frequency region of the resonance Raman spectrum of *Fa.he*. HbF2 at different pH values (Fig. 3, lines a and b). As discussed in the Supplemental material, this relates to a pH-induced change in the out-of-plane distortions of the heme group. Note that similar effects are observed for *Pa. ep*. Hb.

The absorption spectrum of the CO complex of ferrous *Fa.he*. HbF2 at pH 8.5 shows the typical Soret band at 422 nm and the α and β bands at, respectively, 540 and 570 nm

Table 2. *Worm counts and liver damage score of calves vaccinated with* Fasciola hepatica *Hb*

Group	Recovered flukes (% immatures)		Mean liver damage score
	Mean ± SD	Flukes/animal	
Control	110.4 ± 36.9	121, 147, 90, 197, 68, 116, 108, 73, 74	2.2
Vaccine	148.2 ± 29.4	153, 222, 170, 52, 65, 193, 96, 145, 238	2.2

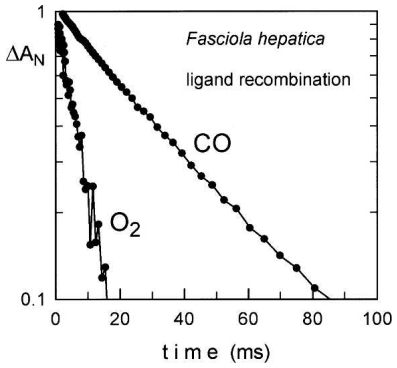

Figure 5. Oxygen and CO binding kinetics of recombinant *Fasciola hepatica* hemoglobin. Absorbance changes are measured at 436 nm. As observed for other trematode Hbs, the ligand binding is quite fast and CO binding is only about three times slower than oxygen, while typical (human) globins show a factor of 10.

(Fig. 2A). Figure 4A presents the low-frequency region of the RR spectra for the CO complex of *Fa.he*. HbF2 in comparison with the CO-ligated form of *Pa.ep*. Hb, previously reported by Das et al. (2006). For the latter case, three frequencies corresponding to the Fe-CO stretching mode ($\nu_{Fe\text{-}CO}$) (at 539, 496, and 479 cm^{-1}) could be identified using isotope labeling. The three frequencies correspond to conformers with different degrees of stabilization of the CO ligand by its surroundings. Although isotope labeling of the CO ligand is required to fully determine the Fe-CO stretching modes of *Fa.he*. HbF2CO, some information can already be obtained from the comparison with the RR spectra of *Pa.ep*. HbCO and from the comparison of the RR spectra taken at different laser powers (hence, different degrees of photo-dissociation of the Fe-CO bond [spectra not shown]). In this way, two possible Fe-CO stretching modes at 496 cm^{-1} and 479 cm^{-1} can be identified in *Fa.he*. HbF2CO (Fig. 4). Marked differences can be observed in the 450–600 cm^{-1} region of *Fa.he*. HbF2CO and *Pa.ep*. HbCO (Fig. 4). The $Fe^{2+}CO$ form characterized by $\nu_{Fe\text{-}CO}$ at 496 cm^{-1} is the so-called *O conformer* (O, open), i.e., an open heme pocket, where no group is close enough to the CO to affect the electronic structure of the Fe-C-O unit (Das et al. 2006). The typical related Fe-C-O bending mode ($\delta_{Fe\text{-}C\text{-}O}$) around 578 cm^{-1} is also observed for *Fa.he*. HbF2CO. The *O conformer* represents a case where ligand escape is not hindered by the surrounding amino acid residues. The lowest Fe-CO stretching frequency (479 cm^{-1}) is assigned to the *N conformer* (N, negative environment), where an interaction between CO and a negatively charged or nonpolar group takes place, i.e., a $Fe - C \equiv O^{\delta+} - X^{-}$ conformation (Das et al. 2000). This conformer has been observed in CO complexes of mutant Mbs and model complexes (Matsu-Ura et al. 2002). It is rarely detected in native heme proteins, and the fact that it is found in the trematode Hbs of *Pa.ep*., *G. crumenifer* (Das et al. 2006) and *Fa.he*. suggests a similar stabilization, most probably by the hydroxyl oxygen of TyrB10 (Das et al. 2006). The third $\nu_{Fe\text{-}CO}$ frequency observed clearly for *Pa.ep*. HbCO (539 cm^{-1}) corresponds to the *C conformer* (C, closed), whereby a positively charged group is present near the Fe-bound CO and a $Fe = C = O - X^{+}$ structure is stabilized. The corresponding Fe-C-O bending mode ($\delta_{Fe\text{-}C\text{-}O}$) is expected around 586 cm^{-1}. The presence of the *C conformer* for *Fa.he*. HbF2CO cannot be confirmed based on the current experiments alone (Fig. 4), although the appearance of a clear peak at 586 cm^{-1} ($\delta_{Fe\text{-}C\text{-}O}$) might indicate that a *C conformer* is also occurring in *Fa.he*. HbF2CO. Stabilization of the CO ligand is most probably realized in the *C conformer* of the trematode hemoglobins by a hydrogen bond to the TyrB10 (Das et al. 2006).

Crystal structure analysis

The *Fa.he*. HbF2 structure matches well the structure of *Pa.ep*. Hb, as implied by the contained RMSD value (1.04 Å) over the protein C_α pairs. On the contrary, because of residue insertions/deletions, a structure overlay of *Fa.he*. HbF2 and sperm whale Mb yields a RMSD of 1.89 Å, limited to 69 matching C_α pairs; a similar RMSD value (1.76 Å, calculated on 65 C_α pairs) is reported for the structural overlay of *Fa.he*. HbF2 on the nematode *A. suum* Hb. In both cases the structural differences are distributed over the whole protein backbone and include different tilting of the heme in its crevice.

The distal site of the crystallized *Fa.he*. HbF2 hosts an O_2 molecule coordinated to the heme-Fe atom (Fe–O coordination distance 1.96 Å) and stabilized, as expected, by a direct hydrogen bond to TyrB10 (Fig. 6). Moreover, a distal-site buried water molecule bridges, through hydrogen bonds, TyrB10, ThrE10, and the carbonyl atom of TyrE7. Such sets of distal-site polar interactions match closely those observed in *Pa.ep*. Hb, including the heme cavity hydrogen-bonded water molecule. TyrE7 is oriented in the direction of the CD region, thus not being available for stabilization of the heme ligand through side-chain hydrogen bonds. Inspection of the heme distal-site 3D structures of *Fa.he*. versus *Pa.ep*. Hbs highlights two main differences worthy of notice. On one hand, the TyrB10 OH group appears shifted in the direction of the heme ligand by about 1.0 Å in the *Fa.he*. HbF2 structure. Such an effect may be related to subtle structural changes distributed over the CD-D-E region of the protein, but also to the presence of the O_2 molecule that may promote TyrB10 side-chain readjustment in *Fa.he*. HbF2 (*Pa.ep*. Hb was crystallized as an aquo-met form, thus hosting a water molecule directly linked to the heme-Fe atom). The

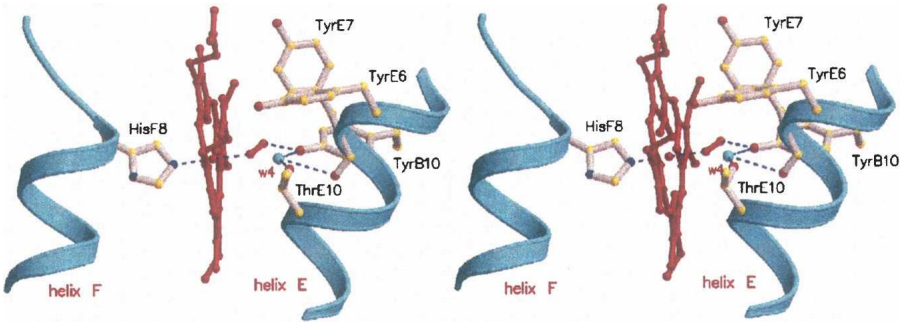

Figure 6. Structure of the *Fa.he*. HbF2 heme pocket. A stereoview of the heme and of the surrounding distal residues contacting the heme and stabilizing the O_2 molecule coordinated to the heme-Fe atom; the proximal HisF8 residue is also shown on the *left* of the heme. Hydrogen bonds within the distal residue cluster, including the heme ligand, are indicated with dashed lines. Water molecule w4 is shown as small (cyan) sphere. Figure drawn with Molscript (Kraulis 1991).

strategic location of the TyrB10 OH group, which appears to be dictated by the hydrogen bond to the distal-site buried water molecule (Wat4, 2.68 Å), results in a short contact to the distal O atom of the heme ligand (2.45 Å). Simple stereochemical considerations, based on the directionality of hydrogen bonds and to the mutual locations of ThrE10, Wat4, and TyrB10 OH group indicate that the latter residue may not be hydrogen bonded to the heme-bound dioxygen. Rather, the TyrB10 OH group may be pointing the electronic lone pairs of the phenolic O atom in the direction of the distal O atom of the heme-bound dioxygen, destabilizing the liganded species because of the short contact between the two O atoms (see Fig. 6). A similar structural arrangement is reminiscent of that observed in *Cerebratulus lacteus* mini-Hb, where the ThrE11 → Val mutation, based on very similar stereochemical/electronic reasons, has a dramatic effect on the O_2-dissociation rate (Pesce et al. 2004).

A second structural issue concerns residue E6, which is Tyr in *Fa.he*. HbF2 vs. His in *Pa.ep*. Hb. In *Fa.he*. HbF2 TyrE6 is involved in hydrogen bonding to the heme A-propionate and together with TyrE7, which is hydrogen bonded to the heme B-propionate, may build a barrier to the diffusion of ligands to the heme through the so-called ''E7 gate,'' shown to be operative in sperm whale Mb (Bolognesi et al. 1997). In *Pa.ep*. Hb the smaller His residue at the E6 site does not allow hydrogen bonding to the heme propionate, and the E7 gate in this case therefore appears more open to ligand diffusion. Such structural property is in keeping with the higher ligand-association rate observed for *Pa.ep*. Hb relative to *Fa.he*. HbF2.

In *Fa.he*. HbF2 the proximal HisF8 residue is properly coordinated to the heme-Fe atom (2.07 Å coordination bond) and is fully staggered relative to the porphyrin pyrrole N-atoms, allowing, in principle, a short Fe–HisF8 coordination bond and in-plane location of the Fe atom. The HisF8 staggered orientation matches almost exactly that observed in *Pa.ep*. Hb, being similarly defined by a strong hydrogen bond (2.76 Å) of HisF8 ND1 atom to the carbonyl O atom of residue GlyF4. The presence of a Gly residue at site F4 of *Fa.he*. HbF2, as opposed to Tyr in *Pa.ep*. Hb, has no apparent effect on the overall conformation of the F-helix, and is matched by a compensating substitution in the facing residues of the E-helix (Ala → Glu at site E14, in *Fa.he*. HbF2). Despite sequence differences in the few residues following HisF8 (Fig. 1), where *Fa.he*. HbF2 hosts ProFG3, the polypeptide backbones of the two trematode Hbs match closely in the FG hinge region.

Vaccination with Fasciola hepatica *hemoglobin*

Trematode Hbs are potentially useful in vaccination strategies for protecting humans and livestock against parasitic infections. However, no protection against *Fa.he*. infection could be raised by vaccination with its Hb (Table 2). Several elements could be at the base of this negative result. (1) The *Fa.he*. HbF2 used as antigen is a recombinant protein expressed in *E. coli*. Expression in a bacterial system and refolding in vitro of Hbs are well-established methodologies resulting in material indistinguishable from the authentic molecule. No post-translational modifications are implemented by bacterial systems and these may play an important role in the immunological characteristics of a molecule. Except for the N-terminal monoacetylation, no post-translational modifications are present in the *Fa.he*. HbF2, as shown by ESI-MS, so this possibility should be ruled out. (2) The choice of an adjuvant may critically determine the outcome of vaccination, e.g., sheep can be protected with *Fa.he*. GST delivered in FSA, but not in GST delivered in several other adjuvants including QuilA/Squalene Montanide (QA/SM). In contrast, GST delivered in QA/SM was the optimal formulation for cattle (Morrison et al.

1996). For *Fa.he*. HbF2, we here used Quil A/Aphigen/cholesterol as adjuvant, which is known to stimulate the humoral (TH2) and cellular responses (TH1). (3) Dalton et al. (1996) obtained protection (43.8%) against infection by immunization with a Hb fraction (Mr > 200 kD) purified from *Fa.he*. ES products. It is evident that the Hb fraction used by these authors is completely different from trematode Hbs as characterized at present (Rashid et al. 1997; Rashid and Weber 1999; Pesce et al. 2001; Sim et al. 2003; de Guzman et al. 2007). Moreover, proteomic analysis of the ES proteins of *Fa.he*. does not reveal Hb (Mr ~ 16,000) as a major ES product (Jefferies et al. 2001). The protection obtained by Dalton et al. (1996) is therefore most likely due to other protein(s) present in the ''Hb'' fraction.

Materials and Methods

Biological material

Fasciola hepatica (*Fa.he*.) parasitic in bovine liver and *Paramphistomum epiclitum (Pa.ep.)* parasitic in the rumen of the common Indian water buffalo *Bubalus bubalis*, were obtained from a local slaughterhouse, respectively, in Antwerp (Belgium) and Aligarh (India). The trematodes were washed thoroughly with normal saline solution and incubated for 1 h at 37°C in 0.15 M NaCl, 8 mM glucose to make them shed their eggs and gut contents. The trematodes were stored at −80°C until use.

Determination of the globin protein sequences

Fa.he. Hb was purified from frozen worms by a combination of ion-exchange and reversed-phase chromatography as described previously (Rashid et al. 1997). The purified globin was digested with trypsin and the resulting peptides separated by RP-HPLC on a Vydac C4 column (2.1 mm) developed with a 0.1% trifluoroacetic acid/acetonitrile system. Sequencing of the purified peptides was performed on an ABI 471-B or Procise instrument operated as recommended by the manufacturer.

Electron-spray ionization mass spectrometry (ESI-MS) of *Fa.he*. Hb was performed on a Quattro Ultima (Micromass UK, Ltd.). The samples were introduced in 0.2% formic acid. The data were accumulated (3–5 min) while scanning m/z 600–1600 at 8 sec/scan and deconvoluted to present the data on a true mass scale using maximum entropy (MaxEnt) based software. Proteolytic digestion with trypsin and α-chymotrypsin was performed according to the scaled-down method of Wild et al. (2001). After digestion, the peptide mixture was diluted 10-fold in 0.2% formic acid and applied directly into the ESI source. The data were accumulated (5 min) while scanning over the m/z 200–2000 at 8 sec/scan. The mass scale was calibrated using a tryptic digest of 50-fold diluted human blood. Tandem MS was undertaken on single- or double-charged peptide ions selected from the digest mixtures and data accumulated (5–20 min) while scanning from m/z 50 to a value appropriate to the Mr of the peptide. Methane was used as the collision gas (0.015 mbar pressure) and the collision energy was adjusted to suit the peptide (25–60V).

Determination of the cDNA and the genes of the fluke Hbs

Live flukes were frozen and pulverized in liquid nitrogen and RNA was extracted using the microRNA isolation kit from Stratagene. cDNA was synthesized and amplified by RT–PCR using two degenerate primers. A positive fragment was purified and sequenced as described earlier (Dewilde et al. 1996). The 3′ end was obtained by a PCR experiment using a specific forward and oligo d(T). The 5′ end was obtained using 5′-RACE (GIBCO BRL) in conjunction with the specific reverse primers as described. Genomic DNA was prepared using standard methods. The globin gene was amplified using the specific primers in a PCR reaction of 35 cycles of 30 sec at 94°C, 1 min at 50°C, and 2 min at 72°C. The resulting amplicon was subsequently purified and sequenced. The gene of *Pa.ep*. was amplified using specific primers based on the cDNA sequence (Rashid et al. 1997) and performed as for the *Fa.he*. gene. See Supplemental material for more details.

Expression cloning of Fa. he. *HbF2*

The cDNA of the *Fa.he*. HbF2 was cloned into the expression vector pET3a as described before (Dewilde et al. 2001). The recombinant expression plasmid was subsequently transformed into *E. coli* strain BL21(DE3)pLysS and expression was carried out as described before (Dewilde et al. 2001). The collected cells were exposed to three freeze-thaw steps and sonicated until completely lysed. The extract was clarified by low (10 min 10,000*g*) and high (60 min 105,000*g*) speed centrifugation and fractionated by ammonium sulfate precipitation (40% and 90%). The 90% pellet was dialyzed against 50 mM Tris-HCl (pH 7.5) and concentrated by Amicon filtration (PM10). Overexpressed *Fa.he*. HbF2 was, however, not folded, and refolding of the Hb was done as follows: The concentrated sample was made up to 6 M guanidinium hydrochloride and 0.5% DTT and was boiled for 5 min. Insoluble material was removed by centrifugation at 10,000*g* for 10 min. Hemin was dissolved in 0.1 M NaOH and 1/10 diluted with 50mM Tris-HCl (pH 7.5). An excess of hemin solution was added to the solubilized protein. This solution was then dialyzed against 5 mM Tris-HCl (pH 8.5). Precipitate formed during dialysis was removed by centrifugation at 10,000*g* for 10 min. The refolded *Fa.he*. HbF2 solution was concentrated by Amicon filtration (PM10), and passed through a Sephacryl S200 column. The pure *Fa.he*. HbF2 fractions were pooled, concentrated, and stored at −30°C.

Ligand-binding kinetics

The kinetics of ligand binding to the heme iron was measured by the flash-photolysis technique (Uzan et al. 2004). Samples were typically 10 μM protein, equilibrated under oxygen, CO, or an equal mixture of both. The mixed atmosphere allows a measurement of the oxygen-dissociation rate: The initial state is CO bound, since the Hb has a higher affinity for CO, but after photodissociation there is an oxy transient form, since oxygen has a higher association rate. The rate of the return to the CO form allows a determination of the oxygen off rate.

Optical and resonance Raman (RR) measurements

Optical measurements were performed with a CARY-5 UV-Vis-NIR spectrophotometer (Varian). RR measurements were

carried out on an 80-cm DILOR XY-800 Raman scattering spectrometer (Dilor) equipped with a triple monochromator, allowing for multichannel liquid-nitrogen cooled CCD detection. The excitation source was a Kr-ion laser (Spectra Physics 2000) (413.1 nm). The protein solution was stirred at 600 rpm to avoid local heating. Ten spectra were recorded (120 sec/spectrum) and averaged after the removal of cosmic ray spikes by an in-house-developed program. Frequency shifts in the RR spectra were calibrated using acetone-CCl_4 as a reference. The laser power was maintained at 17 mW for the deoxy form and at 1 mW for the oxy and CO forms of the protein.

The deoxy ferrous form of the sample was obtained by addition of an excess of sodium dithionite to the protein in 5 mM Tris buffer, pH 8.5, equilibrated under nitrogen atmosphere. For the pH variation, separate buffer solutions of pH 5.5 (acetate buffer), pH 8.5 (Tris buffer), and pH 10 (glycine-NaOH buffer) were prepared. The concentration of the protein samples used for the UV/Vis (RR) measurements was typically 30 μM (60–150 μM).

Continuous-wave electron paramagnetic resonance (CW EPR)

CW-EPR spectra were recorded on a Bruker ESP300E spectrometer (Bruker BioSpin) (microwave frequency 9.43 GHz) equipped with a gas-flow cryogenic system (Oxford Instruments). All of the spectra were recorded with a microwave power of 10 mW, a modulation frequency of 100 kHz, and modulation amplitude of 0.5 mT. The calibration of the magnetic field was done using an NMR Gaussmeter (BRUKER ER 035 M). All of the EPR spectra were simulated with the EasySpin program (Stoll and Schweiger 2006).

Crystal structure analysis

Recombinant *Fa.he*. HbF2 crystal growth conditions were explored using a locally designed sitting-drop vapor-diffusion automated screening procedure based on 566 different chemical conditions, set up with a robotic apparatus (Genesis RSP100 – Tecan). After inspection of the first screens, conditions leading to the isolation of suitable crystals were refined by manual setups to 30% PEG 4000, 0.2 M Mg-chloride, 0.1 M Na-cacodylate (pH 7.0) using 0.2 M Na-thiocyanate as crystallization additive, at 277 K. The crystals grew in 1 wk to a final size of $0.2 \times 0.1 \times 0.1$ mm^3. X-ray diffraction data collection was performed using 35% PEG 4000, 0.2 M $MgCl_2$, 0.2 M Na-thiocyanate, 0.1 M Na-Cacodylate (pH 7.0) supplemented with 15% glycerol as cryoprotectant at beamline ID14eh1, at 100 K (ESRF, Grenoble). The *Fa.he*. HbF2 crystals diffract up to 1.8 Å resolution and belong to the monoclinic $P2_1$ space group, with unit cell parameters: $a = 26.7$ Å, $b = 59.6$ Å, $c = 42.6$ Å, $\beta = 94.6°$; diffraction data were processed using MOSFLM and SCALA (Evans 1993; Leslie 2003). *Fa.he*. HbF2 structure solution was achieved by molecular replacement, using MOLREP (Vagin and Teplyakov 1997) and the atomic coordinates of *Pa.ep*. Hb (PDB-accession code 1H97) (Pesce et al. 2001) as search model, with side chains truncated to Ala in cases of mismatch between the two amino acid sequences. The *Fa.he*. HbF2 structure (one molecule per asymmetric unit) was then refined using REFMAC5 (Murshudov et al. 1997) to the final R_{factor} value of 18.2%, and R_{free} of 22.5%. Model building/correction was performed with COOT (Emsley and Cowtan 2004). Data collection and refinement statistics for *Fa.he*. HbF2 are reported in Supplemental Table S1. *Fa.he*. HbF2 atomic coordinates and structure factors have been deposited with the Protein Data Bank (Berman et al. 2000), with entry codes 2vyw and r2vywsf, respectively.

Vaccination trial

Eighteen helminth-free calves, between 6 and 8 mo of age, were selected. The animals were allocated into two groups of nine as per randomized block design with blocking based on age. The first group of calves received two treatments with saline, 21 d apart, and to the calves of the vaccine group *Fa.he*. HbF2 was administered twice also, 21 d apart. From day 42 after the first treatment, all calves received ~40 metacercariae (mc)/head per day, three times a week for 6 wk for a total of ~720 mc/head. The study terminated on day 140 when the animals were slaughtered. Livers were collected for recovery of liver fluke from the parenchyma and the bile ducts. Scoring of damage to the liver/bile ducts was recorded to provide further information of gross pathological changes, i.e., 0, normal morphology; 1, mild adverse changes in morphology characterized by evidence of mild thickening throughout the bile ducts; 2, moderate adverse changes in morphology characterized by evidence of thickening throughout the bile ducts or localized patches of marked thickening; 3, severe adverse change in morphology characterized by evidence of marked thickening throughout the bile ducts.

Electronic supplemental material

This section includes additional figures, an explanation on methods and information concerning expression, cloning, and purification of *Fa.he*. HbF2, determination of the primary structure, and the spectroscopic characterizations, together with data on crystal structure analysis and refinement.

Acknowledgment

Dr. A. Rashid is acknowledged for the collection of *Paramphistomum epiclitum* from a slaughterhouse in Aligarh, India. This study was supported by INSERM, University of Paris-XI, by the EU (grant QLG3-CT-2002-01548) and by the Fund for Scientific Research of Flanders (FWO) Grant G.0468. S.D. is a postdoctoral fellow of the FWO. Part of this work was supported by the Italian Ministry for University and Scientific Research Project Firb 2003 "Biologia Strutturale" (contract RBLA03B3KC_005). We are grateful to Dr. Amanda Penco for generous help during the crystallization stages.

References

Amiconi, G., Antonini, E., Brunori, M., Formaneck, H., and Huber, R. 1972. Functional properties of native and reconstituted hemoglobins from *Chironomus thummi thummi*. *Eur. J. Biochem.* **31:** 52–58.

Appleby, C.A. 1962. The oxygen equilibrium of leghemoglobin. *Biochim. Biophys. Acta* **60:** 226–235.

Bashford, D., Chothia, C., and Lesk, A.M. 1987. Determinants of a protein fold. Unique features of the globin amino acid sequences. *J. Mol. Biol.* **196:** 199–216.

Berasain, P., Carmona, C., Frangione, B., Dalton, J.P., and Goni, F. 2000. *Fasciola hepatica*: Parasite-secreted proteinases degrade all human IgG subclasses: Determination of the specific cleavage sites and identification of the immunoglobulin fragments produced. *Exp. Parasitol.* **94:** 99–110.

Berman, H.M., Westbrook, J., Feng, Z., Gilliland, G., Bhat, T.N., Weissig, H., Shindyalov, I.N., and Bourne, P.E. 2000. The Protein Data Bank. *Nucleic Acids Res.* **28:** 235–242.

Blumberg, W.E., Peisach, J., Wittenberg, B.A., and Wittenberg, J.B. 1968. The electronic structure of protoheme proteins. I. An electron paramagnetic resonance and optical study of horseradish peroxidase and its derivatives. *J. Biol. Chem.* **243:** 1854–1862.

Bolognesi, M., Bordo, D., Rizzi, M., Tarricone, C., and Ascenzi, P. 1997. Nonvertebrate hemoglobins: Structural bases for reactivity. *Prog. Biophys. Mol. Biol.* **68:** 29–68.

Carver, T.E., Brantley Jr., R.E., Singleton, E.W., Arduini, R.M., Quillin, M.L., Phillips Jr., G.N., and Olson, J.S. 1992. A novel site-directed mutant of myoglobin with an unusually high O_2 affinity and low autooxidation rate. *J. Biol. Chem.* **267:** 14443–14450.

Cavalier-Smith, T. 1985. Selfish DNA and the origin of introns. *Nature* **315:** 283–284.

Cervi, L., Rubinstein, H., and Masih, D.T. 1996. Involvement of excretion-secretion products from *Fasciola hepatica* inducing suppression of the cellular immune responses. *Vet. Parasitol.* **61:** 97–111.

Dalton, J.P., McGonigle, S., Rolph, T.P., and Andrews, S.J. 1996. Induction of protective immunity in cattle against infection with *Fasciola hepatica* by vaccination with cathepsin L proteinases and with hemoglobin. *Infect. Immun.* **64:** 5066–5074.

Das, T.K., Friedman, J.M., Kloek, A.P., Goldberg, D.E., and Rousseau, D.L. 2000. Origin of the anomalous Fe-CO stretching mode in the CO complex of *Ascaris* hemoglobin. *Biochemistry* **39:** 837–842.

Das, T.K., Samuni, U., Lin, Y., Goldberg, D.E., Rousseau, D.L., and Friedman, J.M. 2004. Distal heme pocket conformers of carbonmonoxy derivatives of *Ascaris* hemoglobin: Evidence of conformational trapping in porous sol-gel matrices. *J. Biol. Chem.* **279:** 10433–10441.

Das, T.K., Dewilde, S., Friedman, J.M., Moens, L., and Rousseau, D.L. 2006. Multiple active site conformers in the carbon monoxide complexes of trematode hemoglobins. *J. Biol. Chem.* **281:** 11471–11479.

De Baere, I., Perutz, M.F., Kiger, L., Marden, M.C., and Poyart, C. 1994. Formation of two hydrogen bonds from the globin to the heme-linked oxygen molecule in *Ascaris* hemoglobin. *Proc. Natl. Acad. Sci.* **91:** 1594–1597.

de Guzman, J.V., Yu, H.S., Jeong, H.J., Hong, Y.C., Kim, J., Kong, H.H., and Chung, D.I. 2007. Molecular characterization of two myoglobins of *Paragonimus westermani*. *J. Parasitol.* **93:** 97–103.

Dewilde, S., Blaxter, M., Van Hauwaert, M.L., Vanfleteren, J., Esmans, E.L., Marden, M., Griffon, N., and Moens, L. 1996. Globin and globin gene structure of the nerve myoglobin of *Aphrodite aculeata*. *J. Biol. Chem.* **271:** 19865–19870.

Dewilde, S., Blaxter, M., Van Hauwaert, M.L., Van Houte, K., Pesce, A., Griffon, N., Kiger, L., Marden, M.C., Vermeire, S., Vanfleteren, J., et al. 1998. Structural, functional, and genetic characterization of *Gastrophilus* hemoglobin. *J. Biol. Chem.* **273:** 32467–32474.

Dewilde, S., Kiger, L., Burmester, T., Hankeln, T., Baudin-Creuza, V., Aerts, T., Marden, M.C., Caubergs, R., and Moens, L. 2001. Biochemical characterization and ligand binding properties of neuroglobin, a novel member of the globin family. *J. Biol. Chem.* **276:** 38949–38955.

Di Iorio, E.E., Meier, U.T., Smit, J.D., and Winterhalter, K.H. 1985. Kinetics of oxygen and carbon monoxide binding to liver fluke (*Dicrocoelium dendriticum*) hemoglobin. An extreme case? *J. Biol. Chem.* **260:** 2160–2164.

Emsley, P. and Cowtan, K. 2004. Coot: Model-building tools for molecular graphics. *Acta Crystallogr. D Biol. Crystallogr.* **60:** 2126–2132.

Evans, P.R. 1993. *Proceedings of the CCP4 study weekend, on data collection and processing*. pp 114–122. CLRC Daresbury Laboratory, UK.

Gilbert, W. 1987. The exon theory of genes. *Cold Spring Harb. Symp. Quant. Biol.* **52:** 901–905.

Goldberg, D.E. 1995. The enigmatic oxygen-avid hemoglobin of *Ascaris*. *Bioessays* **17:** 177–182.

Hoogewijs, D., Geuens, E., Dewilde, S., Moens, L., Vierstraete, A., Vinogradov, S., and Vanfleteren, J. 2004. Genome-wide analysis of the globin gene family of *C. elegans*. *IUBMB Life* **56:** 697–702.

Hu, S.Z., Smith, K.M., and Spiro, T.G. 1996. Assignment of protoheme resonance Raman spectrum by heme labeling in myoglobin. *J. Am. Chem. Soc.* **118:** 12638–12646.

Jefferies, J.R., Turner, R.J., and Barrett, J. 1997. Effect of *Fasciola hepatica* excretory-secretory products on the metabolic burst of sheep and human neutrophils. *Int. J. Parasitol.* **27:** 1025–1029.

Jefferies, J.R., Campbell, A.M., van Rossum, A.J., Barrett, J., and Brophy, P.M. 2001. Proteomic analysis of *Fasciola hepatica* excretory-secretory products. *Proteomics* **1:** 1128–1132.

Kiger, L., Rashid, A.K., Griffon, N., Haque, M., Moens, L., Gibson, Q.H., Poyart, C., and Marden, M.C. 1998. Trematode hemoglobins show exceptionally high oxygen affinity. *Biophys. J.* **75:** 990–998.

Kraulis, J. 1991. MOLSCRIPT: A program to produce both detailed and schematic plots of protein structures. *J. Appl. Crystallogr.* **24:** 946–950.

Leslie, A.G.M. 2003. *MOSFLM user guide, Mosflm Version 6.2.3*. MRC Laboratory of Molecular Biology, Cambridge, UK.

Lightowlers, M.W. and Rickard, M.D. 1988. Excretory-secretory products of helminth parasites: Effects on host immune responses. *Parasitology* **96:** S123–S166.

Matsu-Ura, M., Tani, F., and Naruta, Y. 2002. Formation and characterization of carbon monoxide adducts of iron ''twin coronet'' porphyrins. Extremely low CO affinity and a strong negative polar effect on bound CO. *J. Am. Chem. Soc.* **124:** 1941–1950.

McGonigle, S. and Dalton, J.P. 1995. Isolation of *Fasciola hepatica* haemoglobin. *Parasitology* **111:** 209–215.

Minning, D.M., Gow, A.J., Bonaventura, J., Braun, R., Dewhirst, M., Goldberg, D.E., and Stamler, J.S. 1999. *Ascaris* haemoglobin is a nitric oxide-activated ''deoxygenase.''. *Nature* **401:** 497–502.

Morrison, C.A., Colin, T., Sexton, J.L., Bowen, F., Wicker, J., Friedel, T., and Spithill, T.W. 1996. Protection of cattle against *Fasciola hepatica* infection by vaccination with glutathione S-transferase. *Vaccine* **14:** 1603–1612.

Murshudov, G.N., Vagin, A.A., and Dodson, E.J. 1997. Refinement of macromolecular structures by the maximum-likelihood method. *Acta Crystallogr. D Biol. Crystallogr.* **53:** 240–255.

Peisach, J., Blumberg, W.E., Ogawa, S., Rachmilewitz, E.A., and Oltzik, R. 1971. The effects of protein conformation on the heme symmetry in high spin ferric heme proteins as studied by electron paramagnetic resonance. *J. Biol. Chem.* **246:** 3342–3355.

Pesce, A., Dewilde, S., Kiger, L., Milani, M., Ascenzi, P., Marden, M.C., Van Hauwaert, M.L., Vanfleteren, J., Moens, L., and Bolognesi, M. 2001. Very high resolution structure of a trematode hemoglobin displaying a TyrB10-TyrE7 heme distal residue pair and high oxygen affinity. *J. Mol. Biol.* **309:** 1153–1164.

Pesce, A., Nardini, M., Ascenzi, P., Geuens, E., Dewilde, S., Moens, L., Bolognesi, M., Riggs, A.F., Hale, A., Deng, P., et al. 2004. Thr-E11 regulates O_2 affinity in *Cerebratulus lacteus* mini-hemoglobin. *J. Biol. Chem.* **279:** 33662–33672.

Rashid, A.K. and Weber, R.E. 1999. Functional differentiation in trematode hemoglobin isoforms. *Eur. J. Biochem.* **260:** 717–725.

Rashid, A.K., Van Hauwaert, M.L., Haque, M., Siddiqi, A.H., Lasters, I., De Maeyer, M., Griffon, N., Marden, M.C., Dewilde, S., Clauwaert, J., et al. 1997. Trematode myoglobins, functional molecules with a distal tyrosine. *J. Biol. Chem.* **272:** 2992–2999.

Roy, S.W. and Gilbert, W. 2006. The evolution of spliceosomal introns: Patterns, puzzles and progress. *Nat. Rev. Genet.* **7:** 211–221.

Sim, S., Park, G.M., and Yong, T.S. 2003. Cloning and characterization of *Clonorchis sinensis* myoglobin using immune sera against excretory-secretory antigens. *Parasitol. Res.* **91:** 338–343.

Spithill, T.W., Chadee, K., Jardim, A.P., Prichard, R.K., and Ribeiro, P. 2002. Confronting parasites from Canada. *Trends Parasitol.* **18:** 519–521.

Stavrov, S.S. 1993. The effect of iron displacement out of the porphyrin plane on the resonance Raman spectra of heme proteins and iron porphyrins. *Biophys. J.* **65:** 1942–1950.

Stoll, S. and Schweiger, A. 2006. EasySpin, a comprehensive software package for spectral simulation and analysis in EPR. *J. Magn. Reson.* **178:** 42–55.

Uzan, J., Dewilde, S., Burmester, T., Hankeln, T., Moens, L., Hamdane, D., Marden, M.C., and Kiger, L. 2004. Neuroglobin and other hexacoordinated hemoglobins show a weak temperature dependence of oxygen binding. *Biophys. J.* **87:** 1196–1204.

Vagin, A. and Teplyakov, A. 1997. MOLREP: An automated program for molecular replacement. *J. Appl. Crystallogr.* **30:** 1022–1025.

Verity, C.K., McManus, D.P., and Brindley, P.J. 2001. Vaccine efficacy of recombinant cathepsin D aspartic protease from *Schistosoma japonicum*. *Parasite Immunol.* **23:** 153–162.

Wild, B.J., Green, B.N., Cooper, E.K., Lalloz, M.R., Erten, S., Stephens, A.D., and Layton, D.M. 2001. Rapid identification of hemoglobin variants by electrospray ionization mass spectrometry. *Blood Cells Mol. Dis.* **27:** 691–704.

Zhang, W., Rashid, K.A., Haque, M., Siddiqi, A.H., Vinogradov, S.N., Moens, L., and Mar, G.N. 1997. Solution of ^{1}H NMR structure of the heme cavity in the oxygen-avid myoglobin from the trematode *Paramphistomum epiclitum*. *J. Biol. Chem.* **272:** 3000–3006.